American Mineralogist, Volume 105, pages 1593–1597, 2020

Letter

Element loss to platinum capsules in high-temperature–pressure experiments

Jintuan Wang[1,*], Xiaolin Xiong[1,*], Le Zhang[1], and Eiichi Takahashi[1,†]

[1]State Key Laboratory of Isotope Geochemistry, Guangzhou Institute of Geochemistry, CAS, Guangzhou 510640, China

Abstract

Element partition coefficients play key roles in understanding various geological processes and are typically measured by performing high-temperature–pressure (HTP) experiments. In HTP experiments, samples are usually enclosed in capsules made of noble metals. Previous studies have shown that Fe, Ni, and Cu readily alloy with noble metals, resulting in significant loss of these elements from the experimental samples. The loss of elements could severely undermine phase equilibrium and compromise the validity and accuracy of the obtained partition coefficients. However, it remains unclear if other elements (in addition to Fe, Ni, and Cu) will also be lost from samples during HTP experiments, and how to minimize such losses. We performed a series of experiments at 1 GPa and 1400 °C to investigate which elements will be lost from samples and explore the influence of capsule materials and oxygen fugacity (f_{O_2}) on the loss behavior of elements. The starting material is a synthesized basaltic glass consisting of 8 major elements and 37 trace elements. The sample capsules included platinum (Pt), graphite-lined Pt, and rhenium-lined Pt, and the experimental oxygen fugacity (f_{O_2}) was buffered from <FMQ-2 to ~FMQ+5. Results show that: (1) 15 elements (V, Cr, Mn, Fe, Co, Ni, Cu, Zn, Ga, Ge, Cd, In, Sn, W, and Mo) were lost from the sample due to direct contacting and alloying with Pt under graphite-buffered conditions; (2) graphite and Re lining can physically isolate the starting material from Pt and prevent the loss of V, Cr, Mn, Fe, Zn, Ga, Ge, Cd, In, Sn, W, and Mo, but only slightly reduce the loss of Ni and Cu; and (3) element loss can be significantly reduced under oxidizing conditions, and all elements except Cu were retained in the samples under Ru–RuO_2 buffered conditions. These findings provide several viable capsule assemblies that are capable of preventing or reducing element loss, which may prove useful in determining accurate partition coefficients in HTP experiments.

Keywords: Element loss, high-temperature–pressure experiments, capsule materials, experimental f_{O_2}

Introduction

The partitioning behavior of elements is critical to our understanding of various geological processes, including partial melting of rocks in the mantle and crust (Foley et al. 2002; Matzen et al. 2013, 2017; Rapp et al. 2003; Sobolev et al. 2005, 2007; Xiong 2006; Xiong et al. 2005, 2011), fractional crystallization of magmas (Davidson et al. 2007; Lee and Tang 2020; Li et al. 2017), ore formation in magmatic–hydrothermal systems (Liu et al. 2015; Zajacz et al. 2011, 2012, 2017), and the redox state of magmas and their sources (Canil 1997; Lee et al. 2005; Wang et al. 2019). Element partition coefficients between mineral and melt (*D* values) are typically obtained using two approaches. The first is the phenocryst-matrix method, in which partition coefficients are determined by analyzing the elemental concentrations of phenocrysts and coexisting matrix in natural volcanic rocks (Philpotts and Schnetzler 1970; Portnyagin et al. 2017; Schnetzler and Philpotts 1970). However, the accuracy of the phenocryst-matrix method is influenced by various factors, such as disequilibrium between the phenocrysts and matrix, as well as uncertainties in temperature, pressure, and f_{O_2} conditions. The second approach is HTP experiments, in which coexisting minerals and melt are synthesized at HTP conditions. In a HTP experiment, the temperature, pressure, and f_{O_2} are well controlled, and chemical equilibrium can be approached by extending the duration of the experiments. Thus, HTP experiments have been widely used to determine mineral/melt *D* values. In HTP experiments, samples are usually enclosed in capsules made of noble metals. However, a notorious problem in such experiments is that certain elements, including Fe, Ni, and Cu, are lost from the experimental samples by alloying with the noble metal capsules (Adam and Green 2006; Filiberto et al. 2009; Grove 1981; Merrill and Wyllie 1973; Ratajeski and Sisson 1999). Although Au and Au-Pd capsules suffer less element loss, these materials are only applicable at relatively low temperatures (Kawamoto and Hirose 1994; Ratajeski and Sisson 1999). Element loss in HTP experiments can severely undermine phase equilibrium and compromise the validity and accuracy of measured *D* values (Adam and Green 2006; Fellows and Canil 2012; Liu et al. 2014, 2015; Zajacz et al. 2011, 2012). Though the "pre-saturation" technique works well in minimizing iron loss in Pt (Grove 1981) and copper loss in Au (Zajacz et al. 2011), it remains unclear if other elements (in addition to Fe, Ni, and Cu) will also be lost from experimental samples, and how to prevent or minimize such loss. Here, we investigate the loss behavior of 45 elements in Pt capsule at 1400 °C and 1 GPa, and explore the effects of capsule materials and experimental f_{O_2} on it. Based on the results, we

* E-mail: wangjt@gig.ac.cn. Orcid 0000-0002-6682-9036.
† E-mail: xiongxl@gig.ac.cn. Orcid 0000-0002-6500-1827.

0003-004X/20/0010–1593$05.00/DOI: https://doi.org/10.2138/am-2020-7580

propose new capsule assemblies that minimize element loss from samples during HTP experiments.

Experimental and analytical methods

High-temperature–pressure experiments

A synthesized high-Mg basalt (HMB) was used as the starting material. The HMB glass is composed of 8 major elements (SiO_2, TiO_2, Al_2O_3, FeO, MgO, CaO, Na_2O, and K_2O) and 37 trace elements, including large-ion lithophile elements (Li, B, Rb, Sr, Ba, and Cs), rare earth elements (La, Ce, Pr, Nd, Sm, Eu, Gd, Ho, Yb, Lu, and Y), high field strength elements (Zr, Hf, Nb, Ta, P, Sn, W, and Mo), transition elements (Sc, V, Cr, Mn, Co, Ni, Cu, and Zn), and metalloid elements (Ga, Ge, Cd, and In). The major and trace element composition of the HMB glass is homogeneous (Supplemental[1] Table S1). Details of the synthesizing procedures are described in Wang et al. (2019). The trace element contents range between 15 and 1700 ppm, with most contents being ~70 ppm (Supplemental[1] Table S1).

All of the experiments were conducted at 1 GPa and 1400 °C using a Rockland piston-cylinder apparatus at Guangzhou Institute of Geochemistry, Chinese Academy of Sciences. We used a half-inch assembly that comprises a talc sleeve, pyrex glass, graphite furnace, MgO inserts, and sample capsule. The experimental temperature was controlled using a Eurotherm controller and monitored with a Pt-$Pt_{90}Rh_{10}$ thermocouple (S-type). A friction correction of –13% was applied to the apparatus (Liu et al. 2015). The pressure uncertainty in the experiments was about 0.1 GPa, and the temperature gradient along the sample capsule was <15 °C. For each experiment, the HMB powder was sealed into platinum (Pt) capsules (3.0 mm outer diameter; 2.7 mm inner diameter; 6 mm length) together with 0.8 to 3.7 wt% H_2O. Within the capsules, different sample assemblies and f_{O_2} buffers (Fig. 1) were used to change the capsule materials and buffer the experimental f_{O_2}. The experiments were terminated by turning off the power to the heater. The recovered run products were sectioned, mounted in epoxy resin, and polished. Reflected light microscopy and backscattered electron images show that all of the samples quenched to clear glass (Fig. 1), indicating that the samples were melts during the experiments.

LA-ICP-MS analysis

Trace element concentrations in the starting HMB glass and quenched glasses were analyzed using an ELEMENT XR (Thermo-Fisher Scientific) ICP-MS coupled with a 193 nm Resolution M-50 (Resonetics) laser ablation system at Guangzhou Institute of Geochemistry. Laser ablation was performed with an energy density of 4 J/cm^2, a repetition rate of 5 Hz, and a spot size of 33 μm. For each analysis, the gas blank and sample signal were collected for 20 and 30 s, respectively. Signals of the following isotopes were detected: ^{7}Li, ^{11}B, ^{23}Na, ^{25}Mg, ^{27}Al, ^{29}Si, ^{31}P, ^{39}K, ^{43}Ca, ^{45}Sc, ^{47}Ti, ^{51}V, ^{53}Cr, ^{55}Mn, ^{57}Fe, ^{59}Co, ^{60}Ni, ^{63}Cu, ^{66}Zn, ^{70}Ge, ^{71}Ga, ^{85}Rb, ^{88}Sr, ^{89}Y, ^{90}Zr, ^{93}Nb, ^{98}Mo, ^{111}Cd, ^{115}In, ^{118}Sn, ^{133}Cs, ^{137}Ba, ^{139}La, ^{140}Ce, ^{141}Pr, ^{146}Nd, ^{147}Sm, ^{151}Eu, ^{157}Gd, ^{165}Ho, ^{174}Yb, ^{175}Lu, ^{178}Hf, ^{181}Ta, ^{182}W, and ^{185}Re. Reference materials GSD-1G, BHVO-2G, BCR-2G, NIST 610, and NIST 612 were used as external standards, and the SiO_2 content (46.06 wt%) of the HMB glass was used as the internal standard. It is reasonable to use SiO_2 content as the internal standard because silica is inert under the experimental conditions, and also because we focus on element loss relative to the starting material. We also analyzed TB-1G (Elburg et al. 2005) as an unknown sample. The analytical precision (2σ) measured for TB-1G is better than ±10% for all of the elements. Details of the analytical conditions and data processing procedures are described in Zhang et al. (2019). Analytical results are presented in Supplemental[1] Table S1.

Experimental results and discussion

Time-series experiments

Three experiments (using the capsule assembly shown in Fig. 1a) with different durations were conducted to investigate: (1) which elements will lose from the samples by alloying with the Pt capsule under reducing conditions; (2) how long it takes for the elements to reach equilibrium between metallic Pt and melt. These experiments were buffered by graphite at f_{O_2} < FMQ-2 (Medard et al. 2008). As observed under a binocular stereo-microscope, the

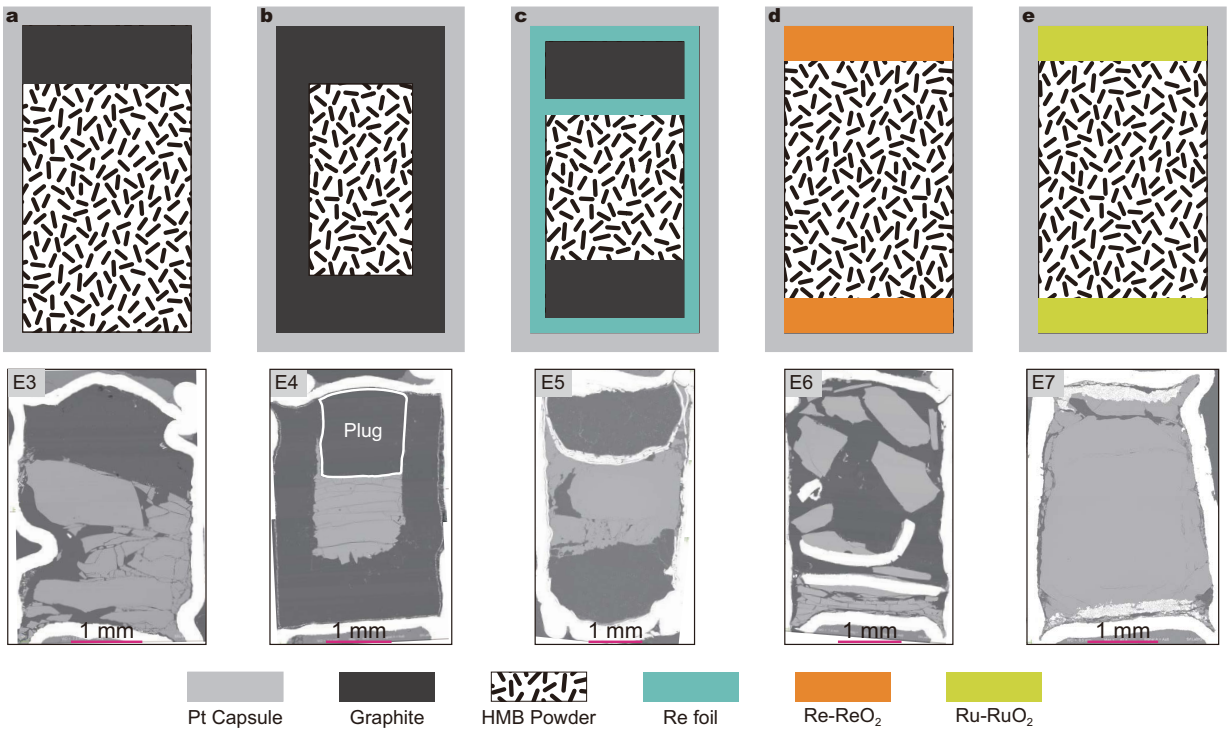

Figure 1. Schematic diagrams showing the sample assemblies inside the Pt capsules (the upper row), and corresponding backscattered electron (BSE) images of the experimental run products (the lower row). The experimental run number is marked in the top left of the BSE images. Note that in E6, the glass breaks into pieces during cutting and therefore it is not present in situ.

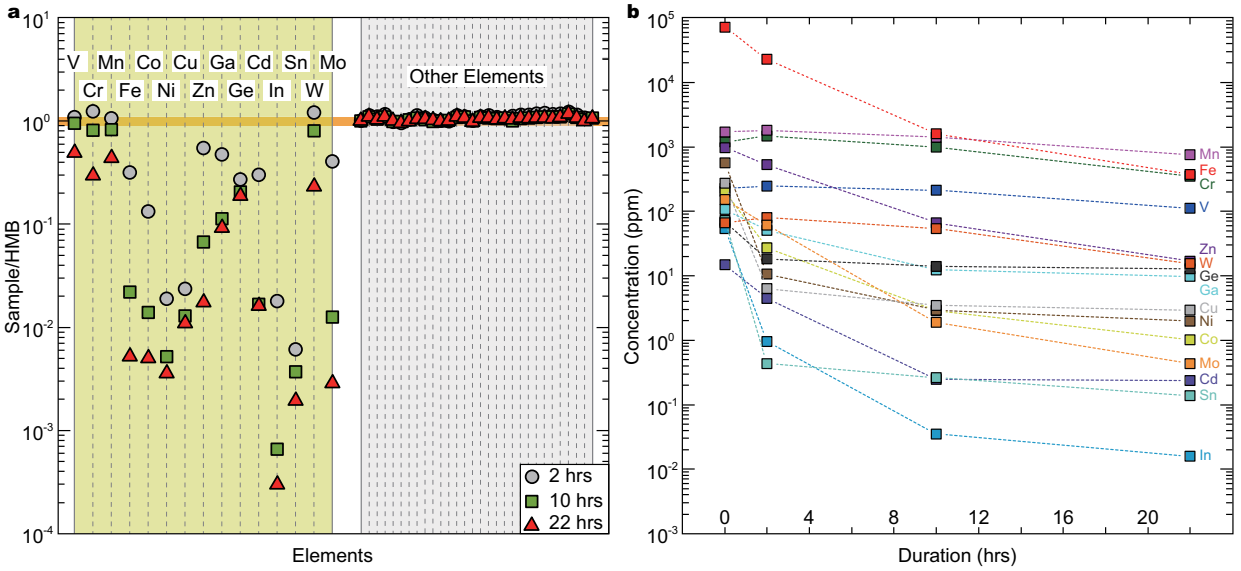

Figure 2. Results of the time-series experiments performed at 1.0 GPa and 1400 °C under reducing conditions (graphite-buffered). (**a**) HMB (starting material)-normalized element concentrations in the experimental run products. The sample/HMB concentration ratios for 15 elements (V, Cr, Mn, Fe, Co, Ni, Cu, Zn, Ga, Ge, Cd, In, Sn, W, and Mo) are <1.0, indicating loss of those elements during the experiments. No loss was observed for other elements, including Si, Al, Mg, Ca, Na, K, P, Sc, Ti, Li, B, Rb, Sr, Ba, Cs, La, Ce, Pr, Nd, Sm, Eu, Gd, Ho, Yb, Lu, Y, Zr, Hf, Nb, and Ta. (**b**) Changes in the concentrations of the 15 elements with experimental duration, which demonstrated that 22 h is sufficient for diffusional equilibrium at the utilized experimental conditions. The 0 h sample represents the starting material.

color of the quenched glasses varies systematically with experimental duration. The glasses changed from dark green after 2 h (E1), to light green after 10 h (E2), and then to nearly transparent after 22 h (E3), suggesting a change in melt composition caused by continuous iron loss. The compositions of quenched glasses (normalized to the starting material) are shown in Figure 2a. We found that 15 elements, including V, Cr, Mn, Fe, Co, Ni, Cu, Zn, Ga, Ge, Cd, In, Sn, W, and Mo, have lower concentrations in the quenched glasses than in the HMB glass, indicating that they were lost from the samples. The concentrations of these 15 elements as a function of experimental duration are plotted in Figure 2b. We found that element concentrations decreased markedly between 0 and 10 h, and then remained nearly constant from 10 to 22 h, demonstrating that these 15 elements approached diffusional equilibrium within 10 h. All experiments described in the following sections were conducted for 22 h to ensure diffusional equilibrium.

The effect of capsule materials

Element loss in the experiments was mainly governed by experimental temperatures, capsule materials, and experimental f_{O_2} values (O'Neill and Nell 1997; Ratajeski and Sisson 1999). Accordingly, it is possible to prevent element loss by changing the capsule materials or by elevating the experimental f_{O_2}. To change the capsule materials, we lined the Pt capsules with graphite and rhenium (Re) foil. In the graphite-lined experiment (E4), the HMB powder was packed into a graphite capsule, which was then placed into the Pt capsule and welded shut (Fig. 1b). We noticed that a robust lining of the Pt capsule is crucial to avoid cracks on the graphite capsule. In the Re-lined experiment (E5), a Re tube and disks were used to insulate the HMB powder from the Pt capsule. We also inserted graphite disks at the bottom and top of the HMB powder to buffer the experimental f_{O_2} (Fig. 1c). Including experiment E3, three samples (all buffered by graphite) encapsulated in a Pt capsule, graphite-lined Pt capsule, and Re-lined Pt capsule, enabled us to investigate the influence of capsule materials on element loss under reducing conditions.

To quantitatively explore the effects of these three capsule materials, we calculated the relative loss of V, Cr, Mn, Fe, Co, Ni, Cu, Zn, Ga, Ge, Cd, In, Sn, W, and Mo in experiments E3, E4, and E5 (Supplemental[1] Table S2). The relative loss of an element denotes the percentage of element loss relative to the starting material and is expressed as follows:

$$\text{Relative Loss} = \frac{C_{STM} - C_{RP}}{C_{STM}} \times 100(\%)$$

where C_{STM} and C_{RP} are the contents of a certain element in the starting material and run products (i.e., quenched glass in this study), respectively. The relative loss can vary from 0% (no element loss) to 100% (complete loss). Here, we divided the relative loss into four grades: no loss (<10%), slight loss (10–30%), moderate loss (30–70%), and severe loss (>70%).

In the case of the Pt capsule (E3) shown in Figure 3a, Fe, Co, Ni, Cu, Zn, Ga, Ge, Cd, In, Sn, W, and Mo are lost severely (relative loss ~100%), whereas V, Cr, and Mn are lost moderately (relative loss >50%). The different relative loss among elements should be governed by the binary metal phase diagram that defines the miscibility between two metals (Hultgren et al. 1973). In the cases of graphite-lined (E4) and Re-lined (E5) Pt capsules, all elements except Co, Ni, and Cu show slight or no loss, suggesting that the graphite and Re lining can effectively prevent element loss (Fig. 3a). The reduced relative loss for most elements in E4 indicates that they were lost to the Pt capsule in E1–E3. The severe

loss of Ni, Cu, and perhaps Co in E4 may be caused by diffusion through the graphite wall to alloy with the Pt capsule, or by reaction with graphite to form carbide. We also note that the concentration of W in E4 is three times higher than in the HMB glass (relative loss = –235), and infer that W contamination may have been introduced by the graphite plug on the top of the capsule (Fig. 1b). This plug was machined from a piece of graphite heater, which turned out to be W-bearing. Other parts of the graphite lining and graphite disks in other experiments were made of spectrum pure graphite. Additionally, the Re-lined capsule performs slightly better than the graphite-lined capsule in reducing Co loss. In summary, by mechanically isolating the samples from the Pt capsule, graphite and Re can prevent the loss of V, Cr, Mn, Fe, Zn, Ga, Ge, Cd, In, Sn, W, and Mo, but do not substantially reduce the loss of Ni and Cu.

The effect of experimental f_{O_2}

The f_{O_2} in two experiments was buffered by loading layers of Re–ReO_2 or Ru–RuO_2 mixtures at the bottom and top of the starting materials (Figs. 1d and 1e), following methods outlined in Armstrong et al. (2019), Mallmann and O'Neill (2007), and Zhang et al. (2017). The redox buffers were made by mixing equal weight proportions of metal and oxides. The ratios of HMB powder to Re–ReO_2 buffer (E6) and Ru–RuO_2 buffer (E7) were 1:1 and 4:1, respectively. After the experiments, the redox buffers contain both metal and oxides, verifying the activity of the buffering reactions. At the experimental conditions investigated here, the calculated f_{O_2} values are ~FMQ+2 for the Re–ReO_2 buffer and ~FMQ+5 for the Ru–RuO_2 buffer (O'Neill and Nell 1997; Pownceby and O'Neill 1994). Including experiment E3, we have three samples using Pt capsules that can be used to investigate the effect of f_{O_2} on the loss behavior of elements (i.e., <FMQ-2, FMQ+2, and FMQ+5).

As shown in Figure 3b, compared with the experiment under reducing conditions (E3; f_{O_2} < FMQ-2), the loss of most elements can be prevented by elevating the experimental f_{O_2}. Only Cu, Ni, Co, In, and Sn were lost at f_{O_2} of ~FMQ+2 (E6; Re–ReO_2 buffer), and only Cu exhibited moderate loss at f_{O_2} of ~FMQ+5 (E7; Ru–RuO_2 buffer). We also observed an extremely high Re concentration (21 792 ± 1974 ppm) in the quenched glass in E6, indicating that the dissolution of ReO_2 occurred. In conclusion, element loss can be prevented by elevating the experimental f_{O_2}. The loss of V, Cr, Mn, Fe, Zn, Ga, Ge, Cd, W, and Mo can be prevented under Re–ReO_2 buffered conditions and all 15 elements except Cu are retained in samples under Ru–RuO_2 buffered conditions.

Implications

Experiments performed at 1.0 GPa and 1400 °C show that: (1) 15 elements, including V, Cr, Mn, Fe, Co, Ni, Cu, Zn, Ga, Ge, Cd, In, Sn, W, and Mo, are readily lost from the experimental samples by alloying with Pt capsules under reducing conditions; (2) graphite- and Re-lined capsules can prevent or substantially reduce the loss of V, Cr, Mn, Fe, Zn, Ga, Ge, Cd, In, Sn, W, and Mo, but do not prevent the loss of Ni and Cu; and (3) element loss can be reduced under oxidizing conditions, and all of the elements investigated here except Cu are retained in the samples under Ru–RuO_2 buffered conditions. These findings have several important implications. First, accurate mineral/melt partition coefficients for most elements (except for Ni and Cu) could be determined by using either graphite-lined or Re-lined capsules, or by elevating the experimental f_{O_2}. Second, partition coefficients

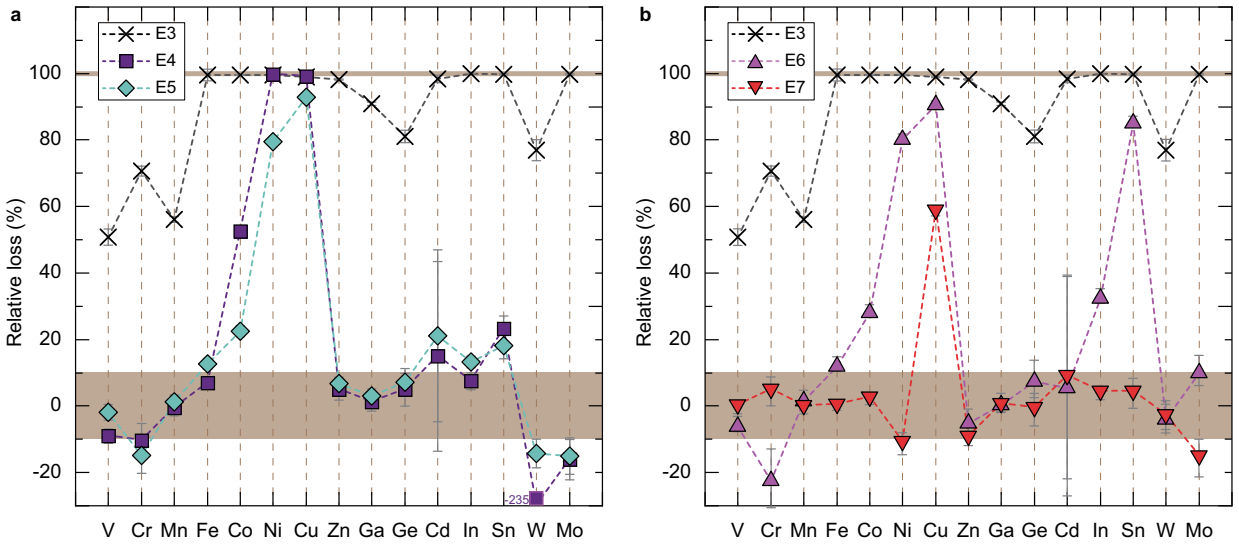

Figure 3. The effects of capsule material and experimental f_{O_2} on the mobility of elements. (**a**) The effect of capsule material on the relative loss of elements under reducing condition (graphite-buffered). In the case of the Pt capsule (E3), the relative loss of the 15 elements is higher than 50 wt%, and Fe, Co, Ni, Cu, Zn, Cd, In, Sn, and Mo were almost lost completely. In the cases of graphite-lined (E4) and Re-lined (E5) Pt capsules, only Cu, Ni, and Co were severely lost. Note that there was W contamination in E4 due to the graphite plug containing a high concentration of W, resulting in the negative relative loss of W in this experiment. The shaded brown area denotes the region of no element loss in this study (<10%). (**b**) The effect of experimental f_{O_2} on the relative loss of elements in Pt capsule experiments. Most of the 15 elements are lost under reducing conditions (E3; graphite-buffered). This can be prevented by elevating the experimental f_{O_2}: only Cu, Ni, Co, In, and Sn were lost at f_{O_2} of ~FMQ+2 (E6: Re–ReO_2 buffer), and only Cu was lost at f_{O_2} of ~FMQ+5 (E7: Ru–RuO_2 buffer).

for Ni can be obtained under Ru–RuO_2 buffered conditions, while partition coefficients for Cu can only be accurately determined by using Cu-bearing alloy as the sample capsule, as demonstrated by Zajacz et al. (2011) and Liu et al. (2014, 2015). Finally, it is promising to experimentally determine melt/fluid partition coefficients for ore-forming elements by mass-balance calculations under Ru–RuO_2 buffered conditions.

Acknowledgments and Funding

We greatly appreciate the constructive comments by Jon Blundy and John C. Ayers, which have improved many aspects of this work. We also thank Don Baker for the handling of this manuscript. This project was financially supported by the National Key Research and Development Program of China (Grant No. 2018YFA0702704) to Xiaolin Xiong; by the Strategic Priority Research Program (XDB18000000) and President's International Fellowship Initiative (2017VSA001) of the CAS to Eiichi Takahashi. All data supporting the conclusions of this paper can be found at http://dx.doi.org/10.17632/5vvgf8xsgv.1 (Mendeley Data). This is contribution no. IS-2879 from GIGCAS.

References cited

Adam, J., and Green, T. (2006) Trace element partitioning between mica- and amphibole-bearing garnet lherzolite and hydrous basanitic melt: 1. Experimental results and the investigation of controls on partitioning behaviour. Contributions to Mineralogy and Petrology, 152(1), 1–17.

Armstrong, K., Frost, D.J., McCammon, C.A., Rubie, D.C., and Boffa Ballaran, T. (2019) Deep magma ocean formation set the oxidation state of Earth's mantle. Science, 365(6456), 903–906.

Canil, D. (1997) Vanadium partitioning and the oxidation state of Archaean komatiite magmas. Nature, 389, 842–845.

Davidson, J., Turner, S., Handley, H., Macpherson, C., and Dosseto, A. (2007) Amphibole "sponge" in arc crust? Geology, 35(9), 787–790.

Elburg, M., Vroon, P., van der Wagt, B., and Tchalikian, A. (2005) Sr and Pb isotopic composition of five USGS glasses (BHVO-2G, BIR-1G, BCR-2G, TB-1G, NKT-1G). Chemical Geology, 223(4), 196–207.

Fellows, S.A., and Canil, D. (2012) Experimental study of the partitioning of Cu during partial melting of Earth's mantle. Earth and Planetary Science Letters, 337-338, 133–143.

Filiberto, J., Jackson, C., Le, L., and Treiman, A.H. (2009) Partitioning of Ni between olivine and an iron-rich basalt: Experiments, partition models, and planetary implications. American Mineralogist, 94(2-3), 256–261.

Foley, S., Tiepolo, M., and Vannucci, R. (2002) Growth of early continental crust controlled by melting of amphibolite in subduction zones. Nature, 417, 837–840.

Grove, T.L. (1981) Use of FePt alloys to eliminate the iron loss problem in 1-atmosphere gas mixing experiments: Theoretical and practical considerations. Contributions to Mineralogy and Petrology, 78, 298–304.

Hultgren, R., Desai, P.D., Hawkins, D.T., Gleiser, M., Kelley, K.K., and Wagman, D.D. (1973) Selected values of the thermodynamic properties of binary alloys. American Society for Metals, Metals Park, Ohio.

Kawamoto, T., and Hirose, K. (1994) Au-Pd sample containers for melting experiments on iron and water bearing systems. European Journal of Mineralogy, 6(3), 381–386.

Lee, C.T.A., and Tang, M. (2020) How to make porphyry copper deposits. Earth and Planetary Science Letters, 529.

Lee, C.-T.A., Leeman, W.P., Canil, D., and Li, Z.-X.A. (2005) Similar V/Sc systematics in MORB and arc basalts: Implications for the oxygen fugacities of their mantle source regions. Journal of Petrology, 46(11), 2313–2336.

Li, L., Xiong, X.L., and Liu, X.C. (2017) Nb/Ta fractionation by amphibole in hydrous basaltic systems: Implications for arc magma evolution and continental crust formation. Journal of Petrology, 58(1), 3–28.

Liu, X., Xiong, X., Audétat, A., and Li, Y. (2015) Partitioning of Cu between mafic minerals, Fe–Ti oxides and intermediate to felsic melts. Geochimica et Cosmochimica Acta, 151, 86–102.

Liu, X.C., Xiong, X.L., Audetat, A., Li, Y., Song, M.S., Li, L., Sun, W.D., and Ding, X. (2014) Partitioning of copper between olivine, orthopyroxene, clinopyroxene, spinel, garnet and silicate melts at upper mantle conditions. Geochimica et Cosmochimica Acta, 125, 1–22.

Mallmann, G., and O'Neill, H.St.C. (2007) The effect of oxygen fugacity on the partitioning of Re between crystals and silicate melt during mantle melting. Geochimica et Cosmochimica Acta, 71(11), 2837–2857.

Matzen, A.K., Baker, M.B., Beckett, J.R., and Stolper, E.M. (2013) The temperature and pressure dependence of nickel partitioning between olivine and silicate melt. Journal of Petrology, 54(12), 2521–2545.

Matzen, A.K., Wood, B.J., Baker, M.B., and Stolper, E.M. (2017) The roles of pyroxenite and peridotite in the mantle sources of oceanic basalts. Nature Geoscience, 10(7), 530–535.

Medard, E., McCammon, C.A., Barr, J.A., and Grove, T.L. (2008) Oxygen fugacity, temperature reproducibility, and H_2O contents of nominally anhydrous piston-cylinder experiments using graphite capsules. American Mineralogist, 93(11-12), 1838–1844.

Merrill, R.B., and Wyllie, P.J. (1973) Absorption of iron by platinum capsules in high-pressure rock melting experiments. American Mineralogist, 58(1-2), 16–20.

O'Neill, H.St.C., and Nell, J. (1997) Gibbs free energies of formation of RuO_2, IrO_2, and OsO_2: A high-temperature electrochemical and calorimetric study. Geochimica et Cosmochimica Acta, 61(24), 5279–5293.

Philpotts, J.A., and Schnetzler, C.C. (1970) Phenocrys-matrix partition coefficients for K, Rb, Sr and Ba, with applications to anorthosite and basalt genesis. Geochimica et Cosmochimica Acta, 34, 307–322.

Portnyagin, M.V., Mironov, N.L., and Nazarova, D.P. (2017) Copper partitioning between olivine and melt inclusions and its content in primitive island-arc magmas of kamchatka. Petrology, 25(4), 419–432.

Pownceby, M.I., and O'Neill, H.St.C. (1994) Thermodynamic data from redox reactions at high temperatures. IV. Calibration of the Re-ReO_2 oxygen buffer from EMF and NiO+Ni-Pd redox sensor measurements. Contributions to Mineralogy and Petrology, 118, 130–137.

Rapp, R.P., Shimizu, N., and Norman, M.D. (2003) Growth of early continental crust by partial melting of eclogite. Nature, 425(6958), 605–609.

Ratajeski, K., and Sisson, T.W. (1999) Loss of iron to gold capsules in rock-melting experiments. American Mineralogist, 84(10), 1521–1527.

Schnetzler, C.C., and Philpotts, J.A. (1970) Partition coefllcients of rare-earth elements between igneous matrix material and rock-forming mineral phenocrysts-II. Geochimica et Cosmochimica Acta, 34, 331–340.

Sobolev, A.V., Hofmann, A.W., Sobolev, S.V., and Nikogosian, I.K. (2005) An olivine-free mantle source of Hawaiian shield basalts. Nature, 434, 590–597.

Sobolev, A.V., Hofmann, A.W., Kuzmin, D.V., Yaxley, G.M., Arndt, N.T., Chung, S.L., Danyushevsky, L.V., Elliott, T., Frey, F.A., Garcia, M.O., and others. (2007) The amount of recycled crust in sources of mantle-derived melts. Science, 316, 412–417.

Wang, J.T., Xiong, X.L., Takahashi, E., Zhang, L., Li, L., and Liu, X.C. (2019) Oxidation state of arc mantle revealed by partitioning of V, Sc, and Ti between mantle minerals and basaltic melts. Journal of Geophysical Research: Solid Earth, 124(5), 4617–4638.

Xiong, X.L. (2006) Trace element evidence for growth of early continental crust by melting of rutile-bearing hydrous eclogite. Geology, 34(11), 945–948.

Xiong, X.L., Adam, J., and Green, T.H. (2005) Rutile stability and rutile/melt HFSE partitioning during partial melting of hydrous basalt: Implications for TTG genesis. Chemical Geology, 218(3-4), 339–359.

Xiong, X., Keppler, H., Audétat, A., Ni, H., Sun, W., and Li, Y. (2011) Partitioning of Nb and Ta between rutile and felsic melt and the fractionation of Nb/Ta during partial melting of hydrous metabasalt. Geochimica et Cosmochimica Acta, 75(7), 1673–1692.

Zajacz, Z., Seo, J.H., Candela, P.A., Piccoli, P.M., and Tossell, J.A. (2011) The solubility of copper in high-temperature magmatic vapors: A quest for the significance of various chloride and sulfide complexes. Geochimica et Cosmochimica Acta, 75(10), 2811–2827.

Zajacz, Z., Candela, P.A., Piccoli, P.M., Wälle, M., and Sanchez-Valle, C. (2012) Gold and copper in volatile saturated mafic to intermediate magmas: Solubilities, partitioning, and implications for ore deposit formation. Geochimica et Cosmochimica Acta, 91, 140–159.

Zajacz, Z., Candela, P.A., and Piccoli, P.M. (2017) The partitioning of Cu, Au and Mo between liquid and vapor at magmatic temperatures and its implications for the genesis of magmatic-hydrothermal ore deposits. Geochimica et Cosmochimica Acta, 207, 81–101.

Zhang, H.L., Hirschmann, M.M., Cottrell, E., and Withers, A.C. (2017) Effect of pressure on $Fe^{3+}/\Sigma Fe$ ratio in a mafic magma and consequences for magma ocean redox gradients. Geochimica et Cosmochimica Acta, 204, 83–103.

Zhang, L., Ren, Z.Y., Xia, X.P., Yang, Q., Hong, L.B., and Wu, D. (2019) In situ determination of trace elements in melt inclusions using laser ablation inductively coupled plasma sector field mass spectrometry. Rapid Communications in Mass Spectrometry, 33(4), 361–370.

Manuscript received April 29, 2020
Manuscript accepted June 17, 2020
Manuscript handled by Don Baker

Endnote:

[1]Deposit item AM-20-107580, Supplemental Material. Deposit items are free to all readers and found on the MSA website, via the specific issue's Table of Contents (go to http://www.minsocam.org/MSA/AmMin/TOC/2020/Oct2020_data/Oct2020_data.html).